Digest Journal of Nanomaterials and Biostructures Vol. 11, No. 2, April - June 2016, p. 559 - 566

A GENERAL METHOD FOR THE SYNTHESIS OF METAL (Cd, Zn) SULPHIDE NANORODS/GRAPHENE FOR USE AS A HIGH PERFORMANCE PHOTOCATALYST

B. ZENG[a,b,c], X. CHEN[a*]
[a]*College of Mechanical Engineering, Hunan University of Arts and Science, Changde 415000, People's Republic of China*
[b]*College of Materials Science and Engineering, Hunan University , Changsha 410082, People's Republic of China*
[c]*Hunan Collaborative innovation Center for construction and development of Dongting Lake Ecological Economic Zone*

A general method for the synthesis of metal (Cd, Zn) sulphide nanorods/graphene was developed using microwave technique. The reactions involved in photocatalytic degradation of organic pollutant are utilized to measure the photoactivity of the CdS nanorods/graphene and ZnS nanorods/graphene. A significant enhancement in the photoactivity was observed. This method demonstrates a general approach towards the fabrication of various one-dimensional semiconductor/graphene nanocomposites with excellent photocatalytic performance.

(Received October 15, 2015; Accepted May 20, 2016)

Keywords: Graphene; metal (Cd, Zn) sulphide; photocatalytic performance.

1. Introduction

Graphene, a two dimensional (2D) nanosheet of sp2 bonded carbon atoms, manifests large specific surface area, superior electron mobility and offer various potential applications in supercapacitors [1], energy conversion devices [2], electrocatalysis [3] and photocatalysis [4].

As a green technology for nonselective degradation of pollutants, in both liquid and gas phases, photocatalysis is currently a topic of particular concern [5]. Owing to their excellent photocatalytic properties, CdS and ZnS have increasingly attracted attention, with much effort being devoted to the controllable synthesis of CdS and ZnS nanostructures [6,7]. With their high length-to-diameter ratio and excellent crystallinity, nanorods of CdS and ZnS can offer superior, fast, and long-distance electron transport properties [8,9]. They are expected to exhibit an improved photo-activity in the photocatalytic reaction. Therefore, CdS nanorods (CdS NR) and ZnS nanorods (ZnS NR) are considered as a class of novel photocatalysts.

Owing to a promoted photo-activity, the integration of CdS NR/graphene (CdS NR-G) and ZnS NR/graphene (ZnS NR-G) has always been adopted a mean for improving utilization efficiency of photogenerated electrons in the photocatalytic reactions [10,11]. Up to now, some work related to CdS NR-G and ZnS NR-G nanocomposites have already been reported. For example, Shao et al. exploited one-dimensional CdS/graphene nanocomposites via solvothermal route, which displayed distinctly enhanced photocatalytic activities [12]. Kim et al. developed ZnS nanowires/graphene composites by the thermal chemical vapor deposition method and their excellent optical properties are expected to enable them to be applicable in highly efficient photocatalysis [13]. Thus, the deposition of CdS NR or ZnS NR onto graphene have provided some invigorating perspectives for the further development of photocatalysis. However, so far a general method for the synthesis of CdS NR-G or ZnS NR-G has not been reported.

* Corresponding author: 240939138 @qq.com

Herein, we report a simple and general approach towards the synthesis of metal (Cd, Zn) sulphide nanorods/graphene. The merits of both the components in these novel nanocomposites are exploited. Graphene renders a desirable conductive supporting matrix, whereas the metal (Cd, Zn) sulphide nanorods imparts an effective electron transport capability. It is expected that these methods will open up a new way of synthesizing one-dimensional semiconductor/graphene nanocomposites with excellent photocatalytic activities.

2. Experimental section

2.1 Synthesis of graphene oxides (GO)

Initially, 3 g of both graphite powder and sodium nitrate were added into 150 ml of concentrated H_2SO_4, kept under an ice bath. Followed by this, 9 g of $KMnO_4$ was slowly added. Later on, the mixture was stirred for about 2 h at 40 ℃. As a next step, 150 ml of deionized water was added into the mixture, and the temperature was raised to 98 ℃. Shortly after 20 min of stirring, 30 ml of 35% H_2O_2 solution was added to the mixture. The solution was then filtered, and washed with 1:10 HCl aqueous solution until the pH turned 7. Lastly, the suspension was dried in a vacuum oven at 60 ℃, and a yellowish powder was obtained as end product.

2.2 Synthesis of CdS NR-G nanocomposites.

30 ml of octylamine, with a specific amount of GO added to it, was stirred for 1 h. 0.266 g of $Cd(AC)_2$ and 0.075 g of thioacetamide (TAA) were added into the above solution, followed by 30 min of vigorous stirring. Then, the blended suspension was heated for 60 min using microwave heating and a yellowish precipitation was achieved. The precipitation was collected by centrifugation, followed by washing with ethanol, and drying at room temperature. The GO to $Cd(AC)_2$ weight ratios opted were 0%, 2%, 4%, and 6% with the corresponding as-prepared samples labeled as CdS NR, CdS NR-G2 , CdS NR-G4, and CdS NR-G6, respectively.

2.3 Synthesis of ZnS NR-G nanocomposites.

30 ml of octylamine, along with 0.002 g of GO, was stirred for 30 min. 0.183 g $Zn(AC)_2$ and 0.075 g thioacetamide (TAA) were dissolved in the above solution and stirred for 30 min. Then, the blended suspension was heated for 60 min using microwave heating, which was followed by a grey precipitation. The precipitation was collected by centrifugation, and washed with ethanol, followed by drying at room temperature. The as-prepared samples were labeled as ZnS NR-G.

2.4 Characterization

The phases of the as-prepared samples were identified by powder X-ray diffraction (XRD, D5000). Morphology of the products were determined by Scanning Electron Microscopy (SEM, S4800) and Transmission Electron Microscopy (TEM, JEM-2100F). Fourier transform infrared spectra were obtained on a WQF-410. The compositions and chemical states of the nanocomposites were examined by X-ray photoelectron spectroscopy (XPS, K-Alpha 1063). Electrochemical impedance spectroscopy (EIS) experiments were performed with a CHI660B workstation according to [14].

2.5 Photocatalytic experiments

20 mg of the as-prepared products were suspended in 20 ml of methyl orange (MO) solution (20 $mg.l^{-1}$). The suspensions were magnetically stirred for 1 h in dark to ensure an adsorption/desorption equilibrium. Next, the solutions were irradiated by either visible or UV light. Later on, 1 ml of the suspension from each composition batch was collected at intervals of 20 min, which, after removing the catalyst nanoparticles, was then analyzed using a UV-vis spectrometer (UV-2550).

3. Results and discussion

XRD is an effective method to analyze the structure and phase of the synthesized materials. As shown in Fig. 1, The peaks at 24.8°, 26.5°, 28.2°, 43.7°, 47.9°, and 52.8° could be assigned to (100), (002), (101), (110), (103), and (201) CdS NR crystal planes respectively (JCPDS No. 41-1049). No characteristic peaks corresponding to GO (001) or graphene (002) planes were observed in CdS NR-G4. This may be attributed to the fact that GO has been reduced to graphene by the microwave heat treatment [15] and that the reduced GO sheets were exfoliated by the deposition of CdS nanorods onto their surfaces [16].

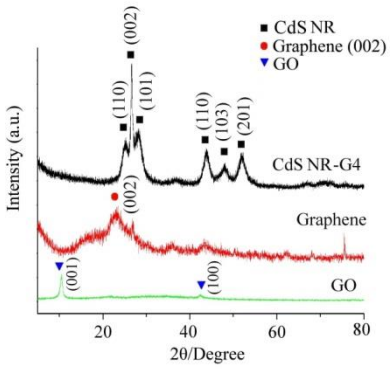

Fig. 1. XRD pattern of GO, graphene and CdS NR-G4.

FTIR spectra is a powerful tool for investigating the effectiveness of the reduction of GO. As shown in Fig. 2, the characteristic absorption peak of GO at 1625 cm^{-1} can be assigned to the in-plane vibrations of sp^2 hybridized C-C bonding. The adsorption peaks at 1074 cm^{-1}, 1396 cm^{-1}, and 1727 cm^{-1} are attributed to the stretching modes of the alkoxy (C-O), the carboxyl (O-H) and the carbonyl (C=O) group respectively [17]. The trivial absorption peak at 3432 cm^{-1} comes from the -OH stretching mode. However, the intensity of all oxygen based functional groups for the CdS NR-G4 sample apparently decreases, indicative of an effective reduction of GO realized by the microwave heat treatment.

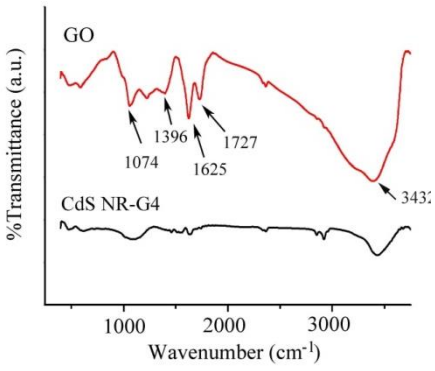

Fig. 2. FTIR spectra of GO and CdS NR-G4.

X-ray photoelectron spectroscopy (XPS) can provide important information about the chemical states of the elements in the CdS NR–G4 end product. The peaks of the full XPS spectra (Fig. 3a) could be attributed to C, O, Cd, and S. Fig. 3b and c shows that the main elements on the surface of the composite are Cd (405.65 eV, 412.2 eV), S (162.05 eV), which is consistent with the literature values [12] for CdS. XPS spectra corresponding to 1s C orbital were investigated for the confirmation of the reduction of GO in CdS-G4 nanocomposite. The characteristic peaks at 284.6

(C=C-C), 286.7 eV (C-O), 287.7 eV (C=O) and 288.9 eV(O-C=O) are identified. As compared to the case of GO [18], oxygenated functional groups in CdS NR-G4 nanocomposite seems to be dramatically decreased, demonstrating that the graphene structure is formed following the microwave heat treatment. It can be presumed that the dominance of the C=C–C peak can favor the efficient electron transport properties in the nanocomposites.

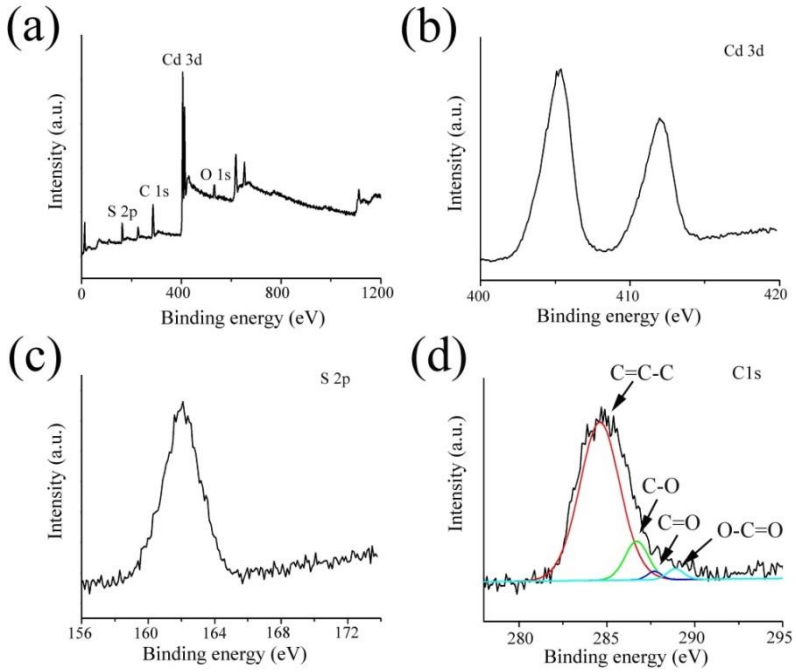

Fig. 3. Typical XPS spectra of the CdS NR-G4 (a) survey spectra, (b) Cd 2d region XPS spectrum, (c) S 2p region XPS spectrum, (d) C 1s region XPS spectrum

In the electrochemical impedance spectroscopy measurements (Fig. 4), the radius of the impedance plot for CdS NR is relatively larger. On the other hand, the semicircle corresponding to CdS NR-G4 electrodes, as seen in the graph, is comparatively smaller, suggesting a much lower charge transfer resistance on the surface of the CdS NR-G4 nanocomposites. This means that the photogenerated electrons from the CdS NR can easily transfer to graphene. Such low charge transfer resistance in CdS NR-G4 may be due to intimate interfacial contact between CdS NR and graphene. Because the conduction band level of CdS NR and graphene are -0.7 V and -0.08 V, respectively, the transferring of photo-electrons from the CdS conduction band to the graphene is favored by the difference in energy levels. As a result, a decreased recombination of electrons and holes can be expected in the photocatalytic reactions.

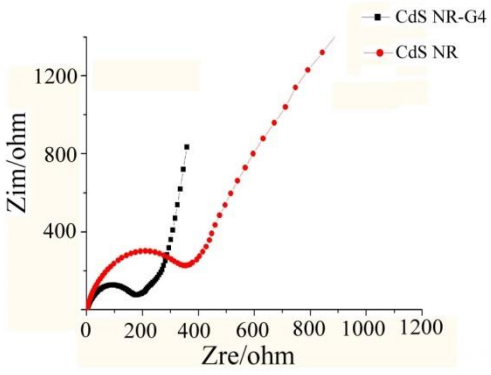

Fig. 4. Nyquist spectra of electrochemical impedance spectra (EIS) for CdS NR and CdS NR-G4.

The morphologies of pristine GO and the CdS NR-G4 nanocomposites have been characterized by SEM, TEM and HRTEM. As shown in Fig. 5a, graphene oxides manifest the 2-D structure of the transparent sheets, with observable presence of ripples on the surface. Fig. 5b is the SEM of CdS NR-G4 nanocomposites and it shows that CdS nanorods are uniformly distributed on the surface of graphene without agglomeration. TEM picture (Fig. 5c) further confirmed 1D morphology of CdS NR with an observable diameter of 5 nm, and a more than 100 nm of aggregate length. From HRTEM image the lattice spacing of 0.336 nm could be estimated from (002) CdS NR plane. These results indicate that graphene can serve as an ideal substrate for distributing CdS NR, while inhibiting their agglomeration. Furthermore, the intimate interfacial contact between graphene and CdS NR in the nanocomposites, is expected to favor charge carrier transfer in the photocatalytic reaction process.

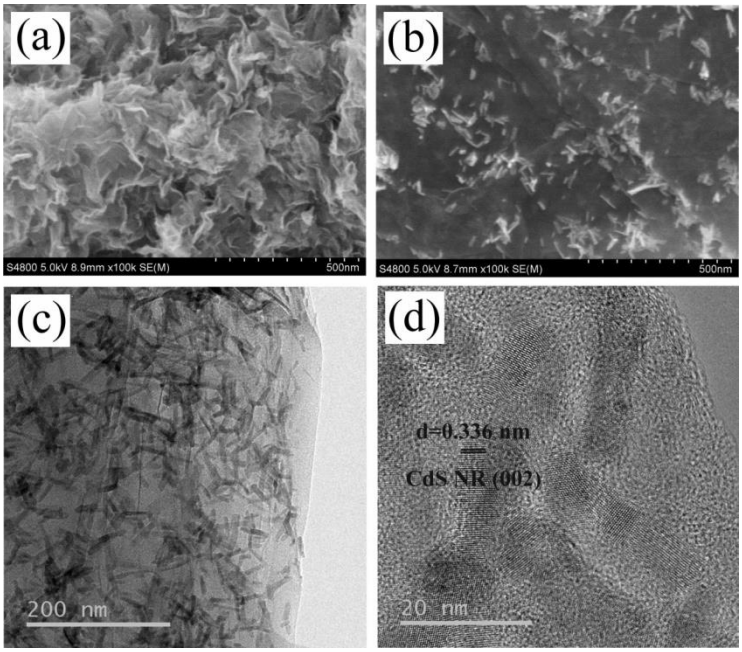

Fig. 5.(a) SEM of GO, (b) SEM, (c) TEM, (d) HRTEM of CdS NR-G4

Fig. 6 shows the profile of MO photodegradation efficiency of different catalysts after 100 minutes of visible light exposure. It can be seen that MO was degraded to 75.6% by CdS NR-G4, while 47.8%, 59.3% and 68.2% MO degradation was achieved using CdS NR, CdS NR-G2, and CdS NR-G6, respectively. The superior photocatalytic performance of CdS NR-G4 can be explained in terms of two main reasons: (1) Compared to the CdS NR, CdS NR-G system could provide a larger specific surface area and hence offer more reaction centers, resulting in an enhancement the photocatalytic activity [19], (2) In the CdS NR-G system, graphene serves as an electron trap at the end of CdS NR, which effectively inhibits any recombination of the photoexcited electron-hole pairs. However, a further increase in the percentage of graphene, simply leads to a decrease in the amount of the active substance, thus negatively affecting catalytic activity of the nanocomposites.

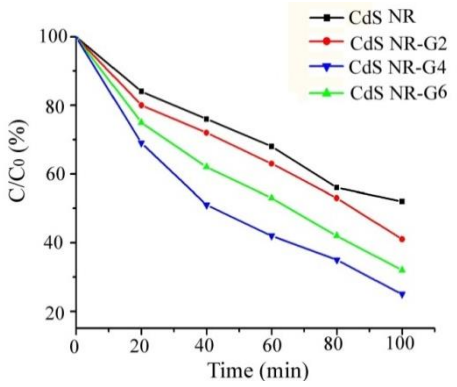

Fig. 6. Photocatalytic degradation efficiency of MO by different catalysts.

The possible photo-degradation mechanism is suggested as shown in Scheme 1 below. Under visible irradiation, the valence electrons of the CdS NR are excited to the conduction band (corresponding positive holes are created in the valence bands), thereby forming the photogenerated electron-hole pairs. Since the conduction band of CdS and graphene are -0.7 V, and -0.08 V respectively [17,20], the photogenerated electrons can easily transfer from CdS NR to the graphene. Thus, graphene can act as an electron trap, which inhibits the recombination of charge carriers, and the photo-induced electrons (transferred from CdS NR to graphene) can subsequently be consumed by the dissolved O_2 to form peroxide radical anions. The active species of peroxide radical anions and the holes in valence band of CdS can oxidize organic pollutants into CO_2 and H_2O. As a result, remarkable photocatalytic activity of CdS NR-G under visible light can be obtained. The possible photocatalytic reaction steps can be summarized by the following equations (1-5);

$$CdS + h\upsilon \rightarrow CdS\ (e^- + h^+) \quad (1)$$

$$CdS\ (e^-) + \text{graphene} \rightarrow CdS + \text{graphene}\ (e^-) \quad (2)$$

$$O_2 + \text{graphene}\ (e^-) \rightarrow O_2^{\cdot -} + \text{graphene} \quad (3)$$

$$CdS\ (h^+) + \text{dye} \rightarrow CdS + CO_2 + H_2O \quad (4)$$

$$O_2^{\cdot -} + \text{dyes} \rightarrow CO_2 + H_2O \quad (5)$$

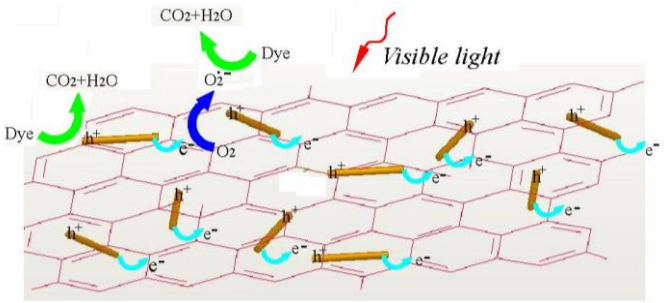

Scheme 1. Schematic diagram of the charge transfer between graphene and CdS nanorods under visible light irradiation

Additionally, we have successfully synthesized ZnS NR-G nanocomposites with the same method. The SEM and TEM images (Fig. 7a and b) reveal that ZnS nanorods of about 50 nm diameter, and more than a few hundreds of nanometers long, are uniformly distributed on the surface of graphene. The XRD pattern (Fig. 7c) confirmed that ZnS and graphene are formed in the nanocomposites. In the light of the photoactivity data, ZnS NR-G exhibited a remarkable photoactivity under UV light illumination, whereby the MO molecules (464 nm) disappeared gradually after a time interval of 30 min (Fig. 7d).

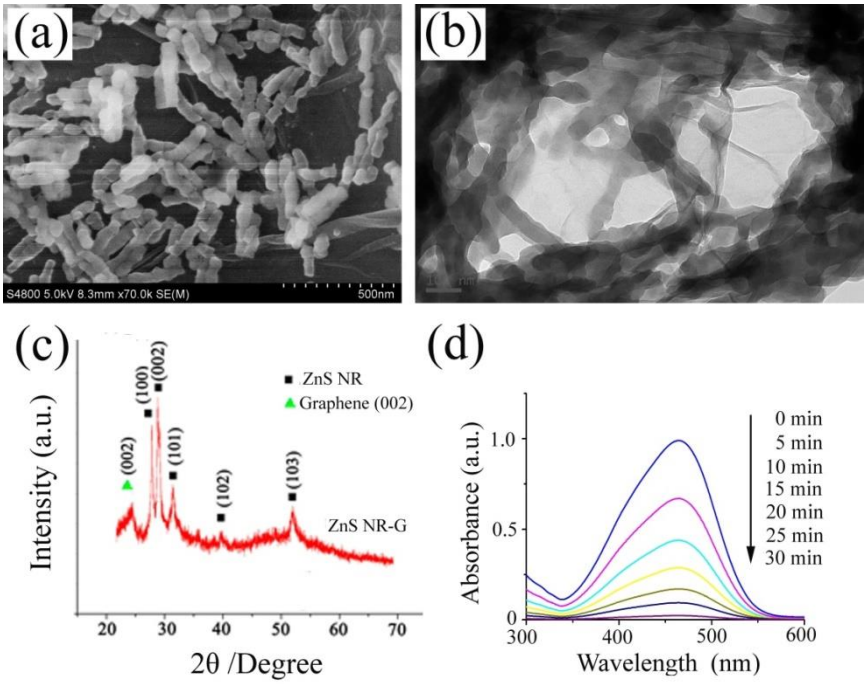

Fig. 7. (a) SEM, (b) TEM, (c) XRD of ZnS NR-G, (d) photocatalytic degradation efficiency

Based on the above experiments, we propose a formation mechanism for metal sulphide nanorods/graphene as shown in scheme 2. With addition of GO into the octylamine followed by stirring for a while, GO suspension could be formed (Scheme 2a). When metal ions and TAA were added to the above suspension, positive metal ions could be anchored onto the surface of GO (due to plenty of oxygen-containing functional groups present) via electrostatic interactions (Scheme 2b) [17]. When the suspension was exposed to microwave irradiation for a short period, ultrathin nanosheet could be formed according to the two-dimensional growth mechanism (Scheme 2c) [17]. With the reaction time increasing, the initially formed ultrathin nanosheets serve as nucleation sites to promote the formation of the next nanosheets (Scheme 2d) [17]. Further prolonging the reaction time, the preferred nucleation on the original nanosheets leads to a layered morphology, forming the metal sulphide nanorods [17]. Meanwhile, GO is reduced to graphene gradually, followed by the color turning from yellow to black (Scheme 2e).

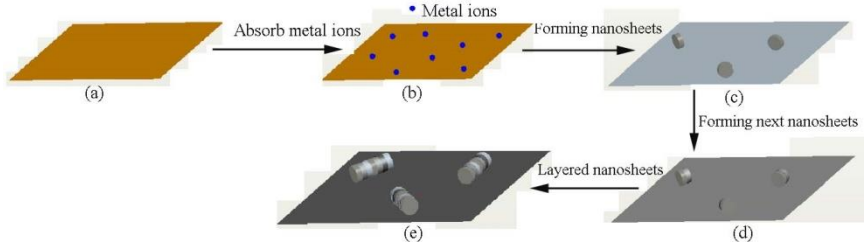

Scheme 2. Schematic illustration for the growth mechanism of metal (Cd, Zn) sulphide nanorods/graphene

4 Conclusions

In summary, we have successfully developed a general method for the synthesis of highly active CdS NR-G and ZnS NR-G nanocomposite photocatalysts. Photocatalytic performance shows that CdS NR-G and ZnS NR-G nanocomposites result in a drastic photoactivity improvement. This superior photocatalytic activity was attributed to the uniform distribution of CdS nanorods and ZnS nanorods onto the graphene sheets, which function as an electron trap and transporter, thereby efficiently promotingseparation of photogenerated charge carriers. The method is environment friendly, economical, and we believe that it can be broadly applied for facile production of other novel one-dimensional nanostructures.

Acknowledgment

This work was supported by the Natural Science Foundation of China (NSFC, No. 50972043), the Construct Program of the Key Discipline in Hunan Province and Project of Hunan Provincial Education Department (15B158).

References

[1] Jun Yan , Qian Wang , Tong Wei, et al. ACS Nano., **8**(5):4720 (2014).
[2] Chuangang Hu, Long Song, Zhipan Zhang et al. Energy and environmental science., **8**, 31 (2015).
[3] Yan Jiao, Yao Zheng, Mietek Jaroniec, et al. Journal of the American chemical society. **136**(11), 4394 (2014).
[4] Zeng Bin, Long Hui. Nano.,**9**(8), 1450097 (2014).
[5] Swagata Banerjee, Suresh C. Pillai , The journal of physical chemistry letters. , **5**(15),2543 (2014).
[6] Bo Weng, Siqi Liu, Nan Zhang, et al. Journal of catalysis, **309**, 146 (2014).
[7] Alexandra A.P. Mansura, Herman S. Mansura, Fábio P. Ramanery, et al. Applied catalysis B: environmental., **158-159**, 269 (2014).
[8] Shuang Cao, Chuanjun Wang, Xiaojun Lv, et al. Applied catalysis B: environmental. **162**, 381 (2015).
[9] ChiJung Chang, Zijing Lee, Chihfeng Wang. International journal of hydrogen energy. **39**(35), 20754 (2014).
[10] Xinjuan Liu, Likun Pan, Tian Lv, et al. Chemical communications.**47**, 11984 (2011).
[11] Jian Cao, Qianyu Liu, Donglai Han, et al. RSC advances, **4**(58), 30798 (2014).
[12] Fengzhen Liu, Xin Shao, Jinqing Wang, et al. Journal of Alloys and Compounds. **551**, 327 (2013).
[13] Sangdan Kim, Hongkyw Choi, Mi Jung, et al. Nanotechnology. **21**, 425203 (2010).
[14] Bin Zeng, Xiaohua Chen, Xutao Ning, et al. Catalysis communications., **43**, 235 (2014).
[15] Lin Ye, Zhaohui Li. Applied batalysis B: environmental.**160-161**, 552 (2014).
[16] Jiaguo Yu,Jian Jin, Bei Cheng, et al. Journal of materials chemistry A.,**2**, 3407 (2014)
[17] Yong Liu, Juncheng. Hu, Tengfei Zhou, et al. Journal of materials chemistry, **21**, 16621 (2011).
[18] Xiaoqiang An, Xuelian Yu, Jimmy C. Yu, et al. Journal of materials chemistry A. **1**, 5158 (2013).
[19] Li Jia, Dong-Hong Wang, Yu-Xi Huang, et al. The journal of physical chemistry C., **115**, 11466 (2011).
[20] Jun Zhang, Jiaguo Yu, Yimin Zhang, et al. Nano letters., **11**, 4774 (2011).